

# Circuit Heating Plant Model with Internal Delays

LIBOR PEKAŘ, ROMAN PROKOP, PETR DOSTÁLEK

Department of Automation and Control

Tomas Bata University in Zlín

Nad Stráněmi 4511, 76005, Zlín

CZECH REPUBLIC

pekar@fai.utb.cz, prokop@fai.utb.cz, dostalek@fai.utb.cz

[http://web.fai.utb.cz/?id=0\\_2\\_2\\_1&lang=en&type=0](http://web.fai.utb.cz/?id=0_2_2_1&lang=en&type=0)

*Abstract:* - The aim of this paper is to utilize an unordinary anisochronic modelling principle on a circuit thermal laboratory plant. The class of anisochronic models is characterized by the existence of state (internal) delays, both distributed or lumped ones. The modelled laboratory appliance was designed at Tomas Bata University in Zlín, Czech Republic, as a thermal heating circuit small scale model with dynamic properties similar to that of a real heating system (e.g. a cooling circuit in cars). The motivation for the modelling of this plant was double. First, the dynamics of the plant exhibits unconventional step responses which cannot be explained by a standard analytic means. Second, the authors of this contribution intend to use the obtained anisochronic mathematical description of the plant with the view of the verification of algebraic control algorithms in the  $R_{MS}$  ring designed for delayed systems earlier.

*Key-Words:* - Anisochronic models, Time-delay systems, Modelling, Heating systems.

## 1 Introduction

Heating (or thermal) systems are still prolific practical industrial as well as real-life applications and they represent a favourite research area as it reveals from recent studies. To name a few, in [1] a method of integral equations for some thermal problems of engineering is proposed (e.g. for radiative heat transfer, heat conduction etc.) which leads to Volterra-Fredholm integrals. Applicable models of pipelines and pipe connections are suggested in [2]. A model of heating system in a room, which is similar to that studied in this paper, is presented in [3]. In [4] a model incorporating internal delays (even of neutral type) for central heating system is presented. However, many of these approaches are a rather complicated and yield distributed parameter models, nearly unusable for a controller design.

The presented contribution deals with anisochronic modelling philosophy introduced already in [5] and subsequently developed for heating systems e.g. in [6-7]. Anisochronic models are characterized by the occurrence of state (internal) delays in a system model. Nevertheless, there are also many industrial processes that include delays in internal feedback loops, e.g. in the model of mass flows in sugar factory [8] or in metallurgic processes [9], to name but a few.

The laboratory heating plant modelled in this paper was assembled at the Faculty of Applied Informatics of Tomas Bata University in Zlín in

order to test control algorithms for systems with dead time. The original description of the apparatus and its electronic circuits can be found in [10]. The motivation for the modelling the plant was double. First, the dynamics of the plant exhibits unconventional step responses which cannot be explained by a standard analytic means. Second, the authors of this contribution intend to use the obtained anisochronic mathematical description of the plant with the view of the verification of algebraic control algorithms in the  $R_{MS}$  ring designed for delayed systems, see e.g. [11-12]

## 2 Description of the Laboratory Heating Model

The plant to be mathematically modelled in this paper was built in order to verify several control algorithms for (conventional) time delay systems. Originally, it was intended to control input delays only; however, as it is shown in this contribution, the plant contains internal delays as well, and thus it is suitable also for testing control approaches for anisochronic systems. The plant dynamics is based on the principle of heat transferring from a source through a piping system using a heat transferring media to a heat-consuming appliance. External appearance of the plant is shown in Fig.1.



Fig.1 – A photo of the laboratory heating model

A schematic sketch of the model is depicted in Fig.2

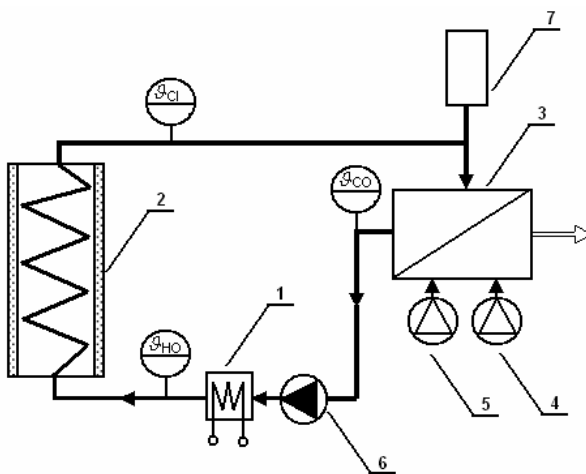


Fig.2 – A scheme of the laboratory heating model

Let us describe the plant according to a schematic sketch depicted in Fig.2. The heat transferring fluid (namely distilled water) is transported using a continuously controllable DC pump {6} into a flow heater {1} with maximum power of 750 W. The temperature of a fluid at the heater output is measured by a platinum thermometer giving value of  $\vartheta_{HO}$ . Warmed liquid then goes through a 15 meters long insulated coiled pipeline {2} which causes the significant delay in the system. The air-water heat exchanger (cooler) {3} with two cooling fans {4, 5} represents a heat-

consuming appliance. The speed of the first fan can be continuously adjusted, whereas the second one is of on/off type. Input and output temperatures of the cooler are measured again by platinum thermometers giving  $\vartheta_{CI}$ , resp.  $\vartheta_{CO}$ . The expansion tank {7} compensates for the expansion effect of the water.

This small scale model can represent dynamics of real heating systems, e.g. a cooling circuit system in cars, heating systems in buildings, etc. The laboratory model is connected to a standard PC via serial bus RS232 and a portable data acquisition unit. All tasks relating to the monitoring and control of the plant are served by software running in Matlab 6.5 environment.

### 3 Anisochronic Model of the Plant

In this section, a possible mathematical model of the plant is proposed. Obviously, an accurate mathematical model of the plant would be rather complicated due to the existence of components causing distributed delays in the system. However, the aim of this contribution is not to find an exact description of the model, but a sufficiently simple mathematical model which can be used for the verification of some control algorithms. Thus, in the following section, the construction of a suitable anisochronic model is proposed. The methodology is based on comprehension of all significant delays and latencies in the model which is built in two steps: First, models of separate functional parts of the plant are found; secondly, separate models are combined by means of their common physical quantities.

Let us introduce notation for process quantities first:

$c$  [ $\text{J kg}^{-1} \text{K}^{-1}$ ] – the specific heat capacity of water

$\dot{m}(t)$  [ $\text{kg s}^{-1}$ ] – the mass flow rate of water

$M_H$  [ $\text{kg}$ ] – the overall mass of water in the heater

$M_C$  [ $\text{kg}$ ] – the overall mass of water in the cooler

$M_P$  [ $\text{kg}$ ] – the overall mass of water in the pipeline

$\vartheta_{HO}(t)$  [ $^{\circ}\text{C}$ ] – output temperature of the heater

$\vartheta_{CI}(t)$  [ $^{\circ}\text{C}$ ] – input temperature of the cooler

$\vartheta_{CO}(t)$  [ $^{\circ}\text{C}$ ] – output temperature of the cooler

$\vartheta_{HI}(t)$  [ $^{\circ}\text{C}$ ] – input temperature of the heater

$\vartheta_A$  [ $^{\circ}\text{C}$ ] – ambient temperature

$P(t)$  [ $\text{W}$ ] – the power of the heater

$\tau_H$  [ $\text{s}$ ] – the delay of a water flow through the heater

$\tau_{HC}$  [ $\text{s}$ ] – the delay of a water flow between the heater and the cooler

$\tau_C$  [s] – the delay of a water flow through the cooler

$\tau_{KC}$  [s] – the delay between a control signal to the cooling fan and the output temperature of the cooler

$\tau_{CH}$  [s] – the delay of a water flow between the cooler and the heater

$u_p(t)$  [V] – a voltage input to the pump

$u_c(t)$  [V] – a voltage input to the cooling fan

$K_H(t)$  [W K<sup>-1</sup>] – the overall heat transmission coefficient of heater wastage energy

$K_C(t)$  [W K<sup>-1</sup>] – the overall heat transmission coefficient of the cooler

$K_p$  [W K<sup>-1</sup>] – the overall heat transmission coefficient of the long pipeline

$h_0, h_1, h_2, h_3, h_4, h_5$  – weighting coefficients for the estimation of the overall heat transmission coefficient of the heater

$c_0$  [W K<sup>-1</sup>],  $c_1$  [W K<sup>-1</sup> V<sup>-1</sup>],  $c_2$  – weighting coefficients for the estimation of the overall heat transmission coefficient of the cooler

$p_0$  [m<sup>3</sup> s<sup>-1</sup>],  $p_1$  [V],  $p_2$  – weighting coefficients for the estimation of the mass flow rate of water

### 3.1 Model of the heater

The energy balance equation is used for the description of the heater

$$cM_H \frac{d\vartheta_{HO}(t)}{dt} = P(t - 0.5\tau_H) + c\dot{m}(t)[\vartheta_{HI}(t - \tau_H) - \vartheta_{HO}(t)] - K_H(t) \left[ \frac{\vartheta_{HO}(t) + \vartheta_{HI}(t - \tau_H)}{2} - \vartheta_A \right] \quad (1)$$

where the arithmetical mean temperature difference is taken for heat losses. and a heating body is assumed to perform heat energy in the middle of the heater. Input temperature,  $\vartheta_{HI}(t)$ , is estimated by “the nearest” measured one,  $\vartheta_{CO}(t)$ , as

$$\vartheta_{HI}(t) = \vartheta_{CO}(t - \tau_{CH}) \quad (2)$$

due to the fact that the fluid transport between the cooler output and the heater input is fast enough so that these two temperatures almost do not differ, except for a time delay. The overall heat transmission coefficient of the heater,  $K_H(t)$ , is numerically approximated by the relation

$$K_H(t) = \frac{h_0 P^2(t) + h_1 \dot{m}^2(t) + h_2 P(t) \dot{m}(t) + h_3}{h_4 P(t) + h_5 \dot{m}(t)} \quad (3)$$

see [13].

### 3.2 Model of the coiled insulated pipeline

A transportation delay in the piping has a decisive influence on the behaviour of the system. Consider the energy balance equation again where heat losses are supposed to be linear along the pipeline

$$cM_p \frac{d\vartheta_{CI}(t)}{dt} = c\dot{m}(t)[\vartheta_{HO}(t - \tau_{HC}) - \vartheta_{CI}(t)] - K_p \left[ \frac{\vartheta_{CI}(t) + \vartheta_{HO}(t - \tau_{HC})}{2} - \vartheta_A \right] \quad (4)$$

Notice that input and output temperatures are not considered in the same time since the thermal effect of the water inlet affects the outlet after some dead time. Heat transmitting coefficient is considered as a low valued constant, thanks to the very good isolation.

The mass of the piping is neglected in the model due to the fact that the specific heat capacity of the material of the pipeline (copper  $\approx 385$  J kg<sup>-1</sup> K<sup>-1</sup>) is much smaller than that of water ( $\approx 4180$  J kg<sup>-1</sup> K<sup>-1</sup>), approximately ten times, and because of the fact that the mass of used copper is lower than that of the fluid (water) inside the piping.

### 3.3 Model of the heat exchanger (cooler)

Time delays in the air-water exchanger are of a distributed nature, thus they have not an important role in system behaviour. On the other hand, the cooler significantly affects the temperature because of its high heat transmission coefficient supported by fans. The energy balance equation reads

$$cM_c \frac{d\vartheta_{CO}(t)}{dt} = c\dot{m}(t)[\vartheta_{CI}(t - \tau_C) - \vartheta_{CO}(t)] - K_C(t) \left[ \frac{\vartheta_{CO}(t) + \vartheta_{CI}(t - \tau_C)}{2} - \vartheta_A \right] \quad (5)$$

The dynamics of the air part of the cooler is much faster in comparison with the water one, thus this dynamics is neglected. The heat transmission coefficient,  $K_C(t)$ , is attempted to be approximated by a function

$$K_C(t) = c_2 u_C^2(t - \tau_{KC}) + c_1 u_C(t - \tau_{KC}) + c_0 \quad (6)$$

Changes in the fan speed affect  $K_c(t)$ . Notice that there is a delay between the control input voltage to the continuously controllable cooling fan,  $u_c(t)$ , and a change of  $K_c(t)$ , in the model. There is no attempt to use models of all electrical and electronics equipments (e.g. the fan motor), and thus coefficients  $c_0, c_1, c_2$  are determined experimentally.

### 3.4 Model of the pump

The influence of the voltage input to the pump,  $u_p(t)$ , upon the mass flow rate of water,  $\dot{m}(t)$ , can be described by a static characteristic

$$\dot{m}(t) = p_0 [u_p(t) + p_1]^{p_2} \quad (7)$$

see [13]. The pump dynamics is omitted comparing to the whole process dynamics. Changes of process delays caused by the change of  $\dot{m}(t)$  are neglected as well, in order to avoid a rather complicated mathematical description of the plant dynamics.

## 4 Model Linearization

From the modelling above, a nonlinear multi-input multi-output (MIMO) model of the plant is obtained. Measured temperatures  $\vartheta_{HO}(t)$ ,  $\vartheta_{CI}(t)$ ,  $\vartheta_{CO}(t)$  are taken as system outputs, whereas analog input voltages  $u_p(t)$ ,  $u_c(t)$  and the power  $P(t)$  are considered as system inputs. To obtain linearized model, the first two terms of the Taylor series expansion at an operation point are used.

From (1)-(3) and (7) one can have

$$\Delta \frac{d\vartheta_{HO}(t)}{dt} \approx A_1 \Delta u_p(t) + \frac{1}{cM_H} \Delta P(t - 0.5\tau_H) \quad (8)$$

$$+ A_2 \Delta P(t) + A_3 \Delta \vartheta_{HO}(t) + A_4 \Delta \vartheta_{CO}(t - \tau_H - \tau_{CH})$$

where

$$A_1 = \left. \frac{\partial}{\partial u_p(t)} \frac{d\vartheta_{HO}(t)}{dt} \right|_0 = \frac{p_0 p_2 (u_{p0} + p_1)^{p_2-1}}{M_H} \left[ \vartheta_{HI0} - \vartheta_{HO0} + (0.5\vartheta_{HI0} + 0.5\vartheta_{HO0} - \vartheta_A) \left( \frac{-h_1 h_5 p_0^2 (u_{p0} + p_1)^{2p_2}}{c [h_5 p_0 (u_{p0} + p_1)^{p_2} + h_4 P_0]^2} + \frac{-2h_1 h_4 P_0 p_0 (u_{p0} + p_1)^{p_2}}{c [h_5 p_0 (u_{p0} + p_1)^{p_2} + h_4 P_0]^2} + \frac{(h_0 h_5 - h_2 h_4) P_0^2 - h_3 h_5}{c [h_5 p_0 (u_{p0} + p_1)^{p_2} + h_4 P_0]^2} \right) \right]$$

$$A_2 = \left. \frac{\partial}{\partial P(t)} \frac{d\vartheta_{HO}(t)}{dt} \right|_0 = \left[ \vartheta_{HI0} - \vartheta_{HO0} + (0.5\vartheta_{HI0} + 0.5\vartheta_{HO0} - \vartheta_A) + \frac{(h_1 h_4 - h_2 h_5) p_0^2 (u_{p0} + p_1)^{2p_2}}{cM_H [h_5 p_0 (u_{p0} + p_1)^{p_2} + h_4 P_0]^2} + \frac{-2h_0 h_5 P_0 p_0 (u_{p0} + p_1)^{p_2} - h_0 h_4 P_0^2 + h_3 h_4}{cM_H [h_5 p_0 (u_{p0} + p_1)^{p_2} + h_4 P_0]^2} \right]$$

$$A_3 = \left. \frac{\partial}{\partial \vartheta_{HO}(t)} \frac{d\vartheta_{HO}(t)}{dt} \right|_0 = -\frac{1}{M_H} \left[ p_0 (u_{p0} + p_1)^{p_2} + \frac{h_1 p_0^2 (u_{p0} + p_1)^{2p_2} + h_2 P_0 p_0 (u_{p0} + p_1)^{p_2}}{2c [h_5 p_0 (u_{p0} + p_1)^{p_2} + h_4 P_0]^2} + \frac{h_0 P_0^2 + h_3}{2c [h_5 p_0 (u_{p0} + p_1)^{p_2} + h_4 P_0]^2} \right]$$

$$A_4 = \left. \frac{\partial}{\partial \vartheta_{CO}(t - \tau_H - \tau_{CH})} \frac{d\vartheta_{HO}(t)}{dt} \right|_0 = \frac{1}{M_H} \left[ p_0 (u_{p0} + p_1)^{p_2} - \frac{h_1 p_0^2 (u_{p0} + p_1)^{2p_2}}{2c [h_5 p_0 (u_{p0} + p_1)^{p_2} + h_4 P_0]^2} + \frac{h_2 P_0 p_0 (u_{p0} + p_1)^{p_2} + h_0 P_0^2 + h_3}{2c [h_5 p_0 (u_{p0} + p_1)^{p_2} + h_4 P_0]^2} \right]$$

Additional index  $(\cdot)_0$  denotes the appropriate quantity value in the steady state (an operation point) and symbol  $\Delta$  stands for deviation from an operation point.

From (4) and (7) we have

$$\Delta \frac{d\vartheta_{CI}(t)}{dt} = A_5 \Delta u_p(t) + A_6 \Delta \vartheta_{HO}(t - \tau_{HC}) + A_7 \Delta \vartheta_{CI}(t) \quad (9)$$

with

$$A_5 = \frac{\partial}{\partial u_p(t)} \frac{d\vartheta_{CI}(t)}{dt} \Big|_0 = \frac{p_2 p_0 (u_{p0} + p_1)^{p_2-1} (\vartheta_{HO0} - \vartheta_{CI0})}{M_P}$$

$$A_6 = \frac{\partial}{\partial \vartheta_{HO}(t - \tau_H)} \frac{d\vartheta_{CI}(t)}{dt} \Big|_0 = \frac{1}{cM_P} [cp_0 (u_{p0} + p_1)^{p_2} - 0.5K_P]$$

$$A_7 = \frac{d}{d\vartheta_{CI}(t)} \frac{d\vartheta_{CI}(t)}{dt} \Big|_0 = -\frac{1}{cM_P} [cp_0 (u_{p0} + p_1)^{p_2} + 0.5K_P]$$

Linearization of (5)-(7) gives

$$\Delta \frac{d\vartheta_{CO}(t)}{dt} = A_8 \Delta u_p(t) + A_9 \Delta u_C(t - \tau_{KC}) + A_{10} \Delta \vartheta_{CO}(t) + A_{11} \Delta \vartheta_{CI}(t - \tau_C) \quad (10)$$

$$A_8 = \frac{\partial}{\partial u_p(t)} \frac{d\vartheta_{CO}(t)}{dt} \Big|_0 = \frac{p_2 p_0 (u_{p0} + p_1)^{p_2-1} (\vartheta_{CI0} - \vartheta_{CO0})}{M_C}$$

$$A_9 = \frac{\partial}{\partial u_C(t - \tau_{KC})} \frac{d\vartheta_{CO}(t)}{dt} \Big|_0 = -\frac{(2c_2 u_{C0} + c_1) p_2 p_0 (u_{p0} + p_1)^{p_2-1}}{cM_C}$$

$$(0.5\vartheta_{CI0} + 0.5\vartheta_{CO0} - \vartheta_A)$$

$$A_{10} = \frac{\partial}{\partial \vartheta_{CO}(t)} \frac{d\vartheta_{CO}(t)}{dt} \Big|_0 = -\frac{1}{cM_P} [2cp_0 (u_{p0} + p_1)^{p_2} + c_2 u_{C0}^2 + c_1 u_{C0} + c_0]$$

$$A_{11} = \frac{\partial}{\partial \vartheta_{CO}(t - \tau_C)} \frac{d\vartheta_{CO}(t)}{dt} \Big|_0 = \frac{1}{cM_P} [2cp_0 (u_{p0} + p_1)^{p_2} - c_2 u_{C0}^2 + c_1 u_{C0} + c_0]$$

A linearized state space model in an operation point then reads

$$\begin{aligned} \begin{bmatrix} \frac{d}{dt} \Delta \vartheta_{HO}(t) \\ \frac{d}{dt} \Delta \vartheta_{CI}(t) \\ \frac{d}{dt} \Delta \vartheta_{CO}(t) \end{bmatrix} &= \begin{bmatrix} A_3 & 0 & 0 \\ 0 & A_7 & 0 \\ 0 & 0 & A_{10} \end{bmatrix} \begin{bmatrix} \Delta \vartheta_{HO}(t) \\ \Delta \vartheta_{CI}(t) \\ \Delta \vartheta_{CO}(t) \end{bmatrix} \\ &+ \begin{bmatrix} 0 & 0 & A_4 \\ 0 & 0 & 0 \\ 0 & 0 & 0 \end{bmatrix} \begin{bmatrix} \Delta \vartheta_{HO}(t - \tau_{CH} - \tau_H) \\ \Delta \vartheta_{CI}(t - \tau_{CH} - \tau_H) \\ \Delta \vartheta_{CO}(t - \tau_{CH} - \tau_H) \end{bmatrix} \\ &+ \begin{bmatrix} 0 & 0 & 0 \\ A_6 & 0 & 0 \\ 0 & 0 & 0 \end{bmatrix} \begin{bmatrix} \Delta \vartheta_{HO}(t - \tau_H) \\ \Delta \vartheta_{CI}(t - \tau_H) \\ \Delta \vartheta_{CO}(t - \tau_H) \end{bmatrix} \\ &+ \begin{bmatrix} 0 & 0 & 0 \\ 0 & 0 & 0 \\ 0 & A_{11} & 0 \end{bmatrix} \begin{bmatrix} \Delta \vartheta_{HO}(t - \tau_C) \\ \Delta \vartheta_{CI}(t - \tau_C) \\ \Delta \vartheta_{CO}(t - \tau_C) \end{bmatrix} \\ &+ \begin{bmatrix} A_1 & 0 & A_2 \\ A_5 & 0 & 0 \\ A_8 & 0 & 0 \end{bmatrix} \begin{bmatrix} \Delta u_p(t) \\ \Delta u_C(t) \\ \Delta P(t) \end{bmatrix} \\ &+ \begin{bmatrix} 0 & 0 & \frac{1}{cM_H} \\ 0 & 0 & 0 \\ 0 & 0 & 0 \end{bmatrix} \begin{bmatrix} \Delta u_p(t - 0.5\tau_H) \\ \Delta u_C(t - 0.5\tau_H) \\ \Delta P(t - 0.5\tau_H) \end{bmatrix} \\ &+ \begin{bmatrix} 0 & 0 & 0 \\ 0 & 0 & 0 \\ 0 & A_9 & 0 \end{bmatrix} \begin{bmatrix} \Delta u_p(t - \tau_{KC}) \\ \Delta u_C(t - \tau_{KC}) \\ \Delta P(t - \tau_{KC}) \end{bmatrix} \\ &\begin{bmatrix} \Delta \vartheta_{HO}(t) \\ \Delta \vartheta_{CI}(t) \\ \Delta \vartheta_{CO}(t) \end{bmatrix} = \begin{bmatrix} 1 & 0 & 0 \\ 0 & 1 & 0 \\ 0 & 0 & 1 \end{bmatrix} \begin{bmatrix} \Delta \vartheta_{HO}(t) \\ \Delta \vartheta_{CI}(t) \\ \Delta \vartheta_{CO}(t) \end{bmatrix} \quad (11) \end{aligned}$$

It should be note that the whole system state is given not only by current values of state variables at time  $t$ , but also by a segment of last system history within the time range  $\langle t - \tau, t \rangle$  where  $\tau = \max\{\tau_C, \tau_{CH} + \tau_H\}$ . Symbol  $\Delta$  for the linearized model is omitted hereinafter. Assuming zero initial

conditions (i.e. steady state in an operation point), the Laplace transform of (11) is given by

$$\begin{bmatrix} \Theta_{HO}(s) \\ \Theta_{CI}(s) \\ \Theta_{CO}(s) \end{bmatrix} s = \begin{bmatrix} A_3 & 0 & A_4 \exp(-(\tau_{CH} + \tau_H)s) \\ A_6 \exp(-\tau_H s) & A_7 & 0 \\ 0 & A_{11} \exp(-\tau_C s) & A_{10} \end{bmatrix} \begin{bmatrix} \Theta_{HO}(s) \\ \Theta_{CI}(s) \\ \Theta_{CO}(s) \end{bmatrix} + \begin{bmatrix} A_1 & 0 & A_2 \frac{\exp(-0.5\tau_H s)}{cM_H} \\ A_5 & 0 & 0 \\ A_8 & A_9 \exp(-\tau_{KC} s) & 0 \end{bmatrix} \begin{bmatrix} U_P(s) \\ U_C(s) \\ P(s) \end{bmatrix} \quad (12)$$

where the capital letters stand for transformed variables denoted with corresponding lower case letters. The transfer matrix of the model thus reads

$$\begin{bmatrix} \Theta_{HO}(s) \\ \Theta_{CI}(s) \\ \Theta_{CO}(s) \end{bmatrix} = \begin{bmatrix} G_{11}(s) & G_{12}(s) & G_{13}(s) \\ G_{21}(s) & G_{22}(s) & G_{23}(s) \\ G_{31}(s) & G_{32}(s) & G_{33}(s) \end{bmatrix} \begin{bmatrix} U_P(s) \\ U_C(s) \\ P(s) \end{bmatrix} \quad (13)$$

$$= \frac{1}{A(s)} \begin{bmatrix} B_{11}(s) & B_{12}(s) & B_{13}(s) \\ B_{21}(s) & B_{22}(s) & B_{23}(s) \\ B_{31}(s) & B_{32}(s) & B_{33}(s) \end{bmatrix} \begin{bmatrix} U_P(s) \\ U_C(s) \\ P(s) \end{bmatrix}$$

where

$$B_{11}(s) = \beta_{11,2} s^2 + \beta_{11,1} s + \beta_{11,1D} s \exp(-\tau_{11,1D} s) + \beta_{11,0} + \beta_{11,0D1} \exp(-\tau_{11,0D1} s) + \beta_{11,0D2} \exp(-\tau_{11,0D2} s)$$

$$B_{12}(s) = (\beta_{12,1} s + \beta_{12,0}) \exp(-\tau_{12} s)$$

$$B_{13}(s) = \beta_{13,2} s^2 + \beta_{13,2D} s^2 \exp(-\tau_{13} s) + \beta_{13,1} s + \beta_{13,1D} s \exp(-\tau_{13} s) + \beta_{13,0} s + \beta_{13,0D} s \exp(-\tau_{13} s)$$

$$B_{21}(s) = \beta_{21,2} s^2 + \beta_{21,1} s + \beta_{21,1D} s \exp(-\tau_{21,1D} s) + \beta_{21,0} + \beta_{21,0D1} \exp(-\tau_{21,0D1} s) + \beta_{21,0D2} \exp(-\tau_{21,0D2} s)$$

$$B_{22}(s) = \beta_{22,0} \exp(-\tau_{22} s)$$

$$B_{23}(s) = [\beta_{23,1} s + \beta_{23,1D} s \exp(-\tau_{23,1D} s) + \beta_{23,0} + \beta_{23,0D} \exp(-\tau_{23,0D} s)] \exp(-\tau_{23} s)$$

$$B_{31}(s) = \beta_{31,2} s^2 + \beta_{31,1} s + \beta_{31,1D} s \exp(-\tau_{31,1D} s) + \beta_{31,0} + \beta_{31,0D1} \exp(-\tau_{31,0D1} s) + \beta_{31,0D2} \exp(-\tau_{31,0D2} s)$$

$$B_{32}(s) = (\beta_{32,2} s^2 + \beta_{32,1D} s + \beta_{32,0}) \exp(-\tau_{32} s)$$

$$B_{33}(s) = [\beta_{33,0D} s \exp(-\tau_{33,0D} s) + \beta_{33,0}] \exp(-\tau_{33} s)$$

$$A(s) = s^3 + \alpha_2 s^2 + \alpha_1 s + \alpha_0 + \alpha_{0D} \exp(-\tau_{0D} s)$$

with

$$\beta_{11,2} = A_1, \beta_{11,1} = -A_1(A_7 + A_{10}), \beta_{11,1D} = A_4 A_8,$$

$$\beta_{11,0} = A_1 A_7 A_{10}, \beta_{11,0D1} = -A_4 A_7 A_8,$$

$$\beta_{11,0D2} = A_4 A_5 A_{11}, \tau_{11,1D} = \tau_{11,0D1} = \tau_{CH} + \tau_H,$$

$$\tau_{11,0D2} = \tau_C + \tau_{CH} + \tau_H$$

$$\beta_{12,1} = A_4 A_9, \beta_{12,0} = -A_4 A_7 A_9, \tau_{12} = \tau_{KC} + \tau_{CH} + \tau_H$$

$$\beta_{13,2} = A_2, \beta_{13,2D} = \frac{1}{cM_H}, \beta_{13,1} = -A_2(A_7 + A_{10}),$$

$$\beta_{13,1D} = -\frac{1}{cM_H}(A_7 + A_{10}), \beta_{13,0} = A_2 A_7 A_{10},$$

$$\beta_{13,0D} = \frac{1}{cM_H} A_7 A_{10}, \tau_{13} = 0.5\tau_H$$

$$\beta_{21,2} = A_5, \beta_{21,1} = -A_5(A_3 + A_{10}), \beta_{21,1D} = A_1 A_6,$$

$$\beta_{21,0} = A_3 A_5 A_{10}, \beta_{21,0D1} = -A_1 A_6 A_{10},$$

$$\beta_{21,0D2} = A_4 A_6 A_8, \tau_{21,1D} = \tau_{21,0D1} = \tau_{HC},$$

$$\tau_{21,0D2} = \tau_{CH} + \tau_H + \tau_{HC}$$

$$\beta_{22,0} = A_4 A_6 A_9, \tau_{22} = \tau_{KC} + \tau_{CH} + \tau_H + \tau_{HC}$$

$$\beta_{23,1} = A_2 A_6, \beta_{23,1D} = A_6 \frac{1}{cM_H}, \beta_{23,0} = -A_2 A_6 A_{10},$$

$$\beta_{23,0D} = -A_6 A_{10} \frac{1}{cM_H}, \tau_{23} = \tau_{HC},$$

$$\tau_{23,1D} = \tau_{23,0D} = 0.5\tau_H$$

$$\beta_{31,2} = A_8, \beta_{31,1} = -A_8(A_3 + A_7), \beta_{31,1D} = A_5 A_{11},$$

$$\beta_{31,0} = A_3 A_7 A_8, \beta_{31,0D1} = -A_3 A_5 A_{11},$$

$$\beta_{31,0D2} = A_1 A_6 A_{11}, \tau_{21,1D} = \tau_{31,0D1} = \tau_C,$$

$$\tau_{31,0D2} = \tau_{HC} + \tau_C$$

$$\beta_{32,2} = A_9, \beta_{32,1} = -A_9(A_3 + A_7), \beta_{32,0} = A_3 A_7 A_9,$$

$$\tau_{32} = \tau_{KC}$$

$$\beta_{33,0D} = A_6 A_{11} \frac{1}{cM_H}, \beta_{33,0} = A_2 A_6 A_{11},$$

$$\tau_{33,0} = 0.5\tau_H, \tau_{33} = \tau_{HC} + \tau_C$$

$$\alpha_2 = -(A_3 + A_7 + A_{10}), \alpha_1 = A_3 A_7 + A_3 A_{10} + A_7 A_{10},$$

$$\alpha_0 = -A_3 A_7 A_{10}, \alpha_{0D} = -A_4 A_6 A_{11},$$

$$\tau_{0D} = \tau_H + \tau_{HC} + \tau_C + \tau_{CH}$$

To demonstrate the structure of anisochronic systems dynamics graphically, a Matlab-Simulink scheme of transfer function  $G_{33}(s)$  is displayed in Fig. 3.

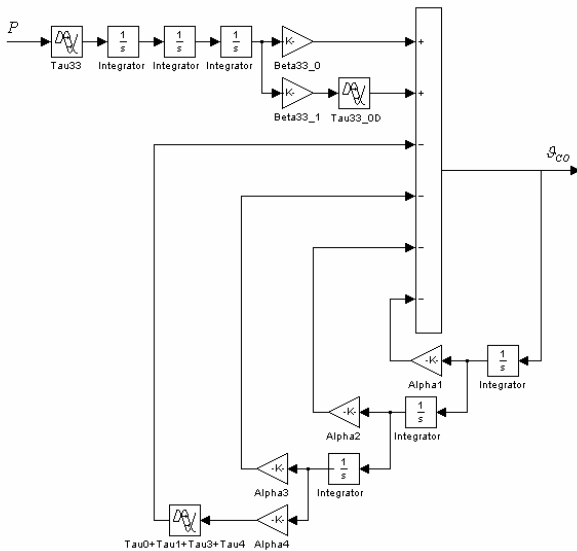


Fig.3 – Matlab-Simulink scheme of transfer function  $G_{33}(s)$

### 5 Parameters Identification

Prior to solving the task of enumeration of model parameters, let us display how unconventional the step response of the system is. Consider the step change of  $P(t)$  resulting in changes of system output temperatures, as it is pictured in Fig.4. An interesting feature of the step response is the existence of “stairs” (“quasi” steady states) in the plot.

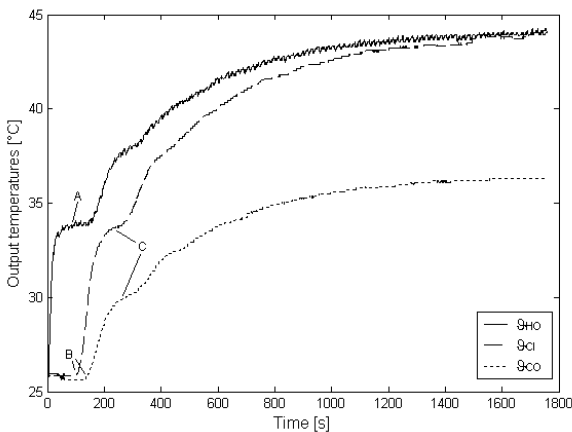


Fig.4 – Heater power step change responses

The existence of these multiple “quasi” steady states can be explained as follows: Temperature of water at the heater output,  $v_{HO}(t)$ , increases until the energy inlet and outlet of the heater equal. In the meanwhile, the “hot” water flow goes through the long pipe to the cooler, and, after some dead-time,  $\tau_{HC}$ , it affects input,  $v_{CI}(t)$ , and output,  $v_{CO}(t)$ , temperatures of the cooler. At this time, the heater input temperature remains constant, because the water flow has not gone a round yet, and  $v_{CO}(t)$  becomes constant. Then “cold” water goes back to the heater and closes a circuit. Again, the closed loop dead time between the cooler output and cooler input,  $\tau = \tau_{CH} + \tau_H + \tau_{HC}$ , is long enough so that  $v_{CI}(t)$  and  $v_{CO}(t)$  become almost constant.

#### 5.1 Estimation of the mass flow rate and the heat transmission coefficient of the heater

There were made no attempts to determinate measure the mass flow rate of water by measuring of the diameter of the pipeline, the water-flow velocity, etc. Steady state data in Table 1 can be used for evaluation of  $\dot{m}(t)$  by taking into account the fact that more than one steady state can be usually found in a step response of the system, see Fig.4.

The steady state of (1) reads

$$0 = P_0 + c\dot{m}_0 [v_{HI0} - v_{H00}] - K_{H0} \left[ \frac{v_{H00} + v_{HI0}}{2} - v_A \right] \tag{14}$$

i.e. the derivative is assumed identically zero. There are two unknown static parameters in (14),  $\dot{m}_0$  and  $K_{H0}$ , for a particular setting of inputs. Mass flow rate,  $\dot{m}(t)$ , as a function of  $u_p(t)$  influences mainly system delays, whereas  $K_H(t)$  given by (3) impresses a “height” of the “first” steady state of  $v_{HO}(t)$ , see Fig.4 (A). Table 2 contains the “first” steady state values of temperatures  $v_{HO}(t)$  and  $v_{HI}(t) = v_{CO}(t - \tau_{CH})$ . These data together with data from Table 1 enable to estimate  $\dot{m}_0$  and  $K_{H0}$  for a particular setting of input values by inserting these data into (14), thus, we have two independent equations (14) for a particular setting of inputs. The final values of  $\dot{m}_0$  and  $K_{H0}$  are taken as the arithmetical mean of all calculated values from these tables for a particular (same) setting. There can be then estimated unknown parameters of  $\dot{m}_0$  and  $K_{H0}$  in (3) and (7), from these values.

Table 1 - Measurements of steady-state temperatures for  $u_c = 3V$

$u_p$ [V]	$P$ [W]	$\vartheta_{H00}$ [°C]	$\vartheta_{C10}$ [°C]	$\vartheta_{C00}$ [°C]	$\vartheta_A$ [°C]
4	225	38.1	38.0	31.3	22
4	225	41.8	41.5	35.1	26
5	225	39.4	39.3	32.9	25
5	225	40.9	40.7	34.5	27
6	225	39.5	39.3	32.9	25.5
6	225	38.0	37.9	33.0	23.5
4	300	43.5	43.2	34.9	25
4	300	42.6	42.5	33.7	23
5	300	41.9	41.8	33.3	22.5
5	300	44.1	43.8	36.0	25
6	300	43.3	42.8	35.2	24
6	300	43.4	43.1	35.3	24
4	375	48.1	47.9	37.1	24
4	375	47.8	47.3	36.8	23.5
5	375	48.8	48.5	38.7	25.5
5	375	49.9	49.7	40.0	26
6	375	48.2	47.8	38.3	23
6	375	49.1	48.9	39.5	26.5
4	400	51.2	50.9	37.7	24
5	400	52.2	52.0	39.9	24
6	400	49.9	49.8	38.2	23

Table 2 - Measurements of “quasi” steady-state temperatures for  $u_c = 3V$

$u_p$ [V]	$P$ [W]	$\vartheta_{H00}$ [°C]	$\vartheta_{H10}$ [°C]	$\vartheta_A$ [°C]
4	225	28.8	21.7	22
4	225	33.0	26.1	26
5	225	31.2	24.7	25
5	225	33.8	26.9	27
6	225	31.8	25.6	25.5
6	225	29.6	23.1	23.5
4	300	33.9	24.5	25
4	300	30.7	21.7	23
5	300	33.9	25.4	25.5
5	300	33.9	25.1	25
6	300	32.1	23.6	24
6	300	32.7	24.1	24
4	375	35.5	24.1	24
4	375	35.3	23.6	23.5
5	375	36.4	25.2	25.5
5	375	36.7	25.7	26
6	375	29.2	22.9	23
6	375	32.8	26.5	26.5
4	400	38.2	23.5	24
5	400	38.9	25.2	24
6	400	36.3	23.3	23

Hence, equation (7) together with data in Table 1 and Table 2 results in  $\dot{m}_0$  as in Table 3, and  $K_{H0}$  as in Table 4, where the water density was chosen as  $\rho = 993 \text{ kg m}^{-3}$ , and  $c = 4180 \text{ J kg}^{-1} \text{ K}^{-1}$ .

Table 3. Measured relation  $\dot{m}_0(u_p)$

$u_p$ [V]	3	4	5	6
$\dot{m}_0$ [ $\text{m}^3 10^{-4}$ ]	69.8	76.1	80.9	83.0

Table 4. Measured relation  $K_{H0}(u_p, P)$  [ $\text{W K}^{-1}$ ]

$P$ [W] \ / $u_p$ [V]	4	5	6
225	1.07	1.37	1.40
300	1.59	1.54	1.24
375	1.46	2.14	2.04
400	2.31	2.76	2.63

The evaluation of these data w.r.t. (3) and (7) results in the following numeric estimation (made in Microsoft Excel Solver):  $h_0 = 8.4925$ ,  $h_1 = -0.0017$ ,  $h_2 = -14999$ ,  $h_3 = -12998$ ,  $h_4 = 1507.988$ ,  $h_5 = 77.766$ ;  $p_0 = 5.077 \cdot 10^{-3}$ ,  $p_1 = 0.266$ ,  $p_2 = 0.274$ . A graphical comparisons of measured and calculated data are in Fig.5 and Fig.6.

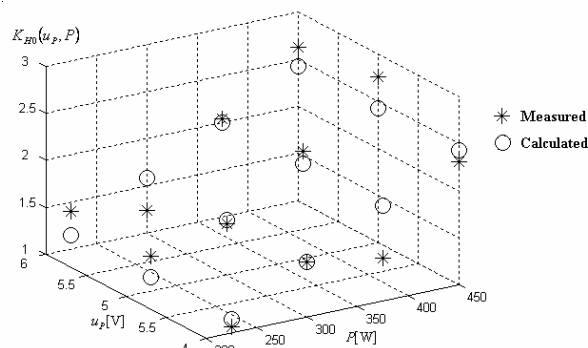


Fig.5 – Comparison of measured and calculated  $K_{H0}$



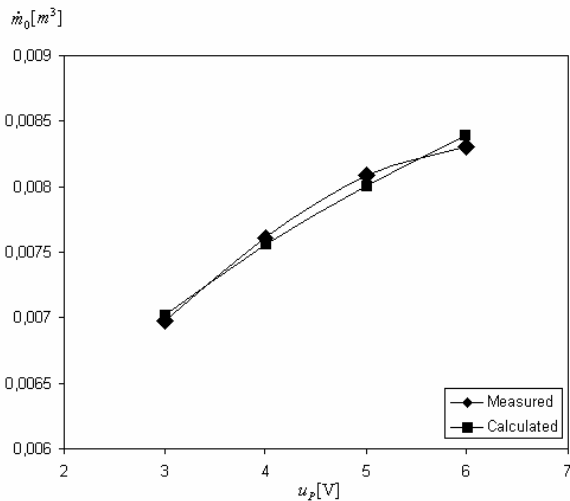


Fig.6 – Comparison of measured and calculated  $\dot{m}_0$

One can see that  $K_{H0}(u_p, P)$  is nearly not depended on the setting of  $u_p$  and thus a linear relation  $K_{H0}(P)$  could be enough to take. The important disadvantage of these estimations is the fact that the results are strongly sensitive to the measurement of the ambient air temperature.

### 5.2 Estimation of the heat transmission coefficient of the coiled insulated pipeline

Data in Table 1 together with the static equation obtained from (4) can be also used for the evaluation of the (constant) heat transmission coefficient  $K_p$  which characterizes especially a “height” of the “quasi” steady state of  $\vartheta_{CI}$ , see Fig. 4 (C). From (4) we have

$$0 = c\dot{m}_0[\vartheta_{H00} - \vartheta_{CI0}] - K_p \left[ \frac{\vartheta_{CI0} + \vartheta_{H00}}{2} - \vartheta_A \right] \quad (15)$$

The final value of  $K_p$  is taken as the arithmetical mean again as  $K_p = 0.39 \text{ W K}^{-1}$ . Obviously, the pipeline is insulated very well and this coefficient does not affect the system dynamics significantly. The measurement is sensitive to  $\vartheta_A$  again, and the A/D converter resolution (cca 0.1 °C) disables to find an more accurate value of  $K_p$ . Moreover, the effect of secondary heating (due to the material of the pipeline) makes a measurement of  $\vartheta_{H00}$  and  $\vartheta_{CI0}$  more difficult.

### 5.3 Estimation of the heat transmission coefficient of the cooler

Steady state yields (5) of the form

$$0 = c\dot{m}_0[\vartheta_{CI0} - \vartheta_{CO0}] - K_{C0} \left[ \frac{\vartheta_{CO0} + \vartheta_{CI0}}{2} - \vartheta_A \right] \quad (16)$$

This equation together with data in Table 5 gives the estimation of  $K_{C0}$ , which characterizes especially a “height” of the “quasi” steady state of  $\vartheta_{CO}(t)$ , see Fig. 4 (C), for a particular setting of  $u_C$ , similarly as in Section 5.1.

Table 5 - Measurements of steady-state temperatures for various  $u_C$ ,  $P = 300 \text{ W}$ ,  $u_p = 5 \text{ V}$

$u_C$ [V]	$\vartheta_{H00}$ [°C]	$\vartheta_{CI0}$ [°C]	$\vartheta_{CO0}$ [°C]	$\vartheta_A$ [°C]
1	48.1	47.9	40.0	24
1	45.3	45.0	36.2	21.5
1	46.5	46.3	38.2	25
2	43.3	42.9	34.7	22.5
2	43.3	42.8	34.9	23.5
2	44.5	44.3	35.8	23
4	39.8	39.3	30.0	20.5
4	42.3	42.2	32.7	23
4	43.1	42.8	34.5	25.5
5	39.6	39.3	31.0	21
5	39.9	39.6	31.6	22
5	40.9	40.6	32.3	24
6	40.6	40.5	32.2	23
6	41.1	40.9	32.6	24.5
6	38.6	38.4	30.2	21

Note: Temperature values for  $u_C = 3 \text{ V}$  are omitted in Table 3 since they can be obtained from Table 1.

The arithmetical mean of particular measured values of  $K_{C0}$  results in relations as in Table 6

Table 6 - Measured relation  $K_{C0}(u_C)$

$u_C$ [V]	$K_{C0}$ [W K <sup>-1</sup> ]
1	14.2
2	16.9
3	18.2
4	19.5
5	21
6	21.4

With help of the numerical optimization (MS Excel) one can obtain coefficients of (6) as

$$c_0 = 11.8, c_1 = 2.755, c_2 = -0.19 \quad (17)$$

A graphical comparison of measured and calculated  $K_{C0}(u_c)$  is in Fig.7.

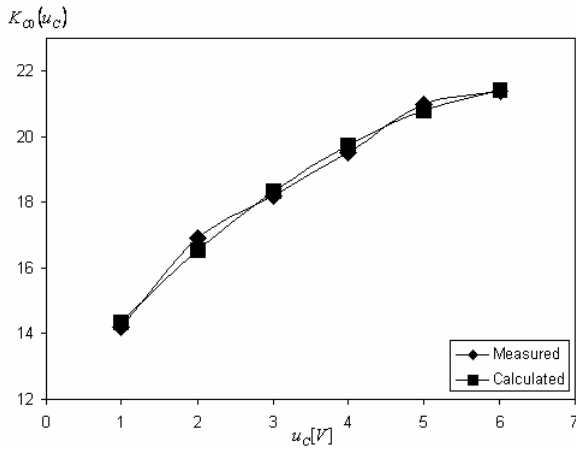


Fig.7 – Comparison of measured and calculated  $K_{C0}$

### 5.4 Static characteristics

All the above presented data enable to draw up the static characteristics of the studied model. Static relations between  $u_p$  and all output temperatures, for  $P = 300 \text{ W}$ ,  $u_c = 3 \text{ V}$ ,  $\vartheta_A = 24^\circ\text{C}$ , are displayed in Fig. 8

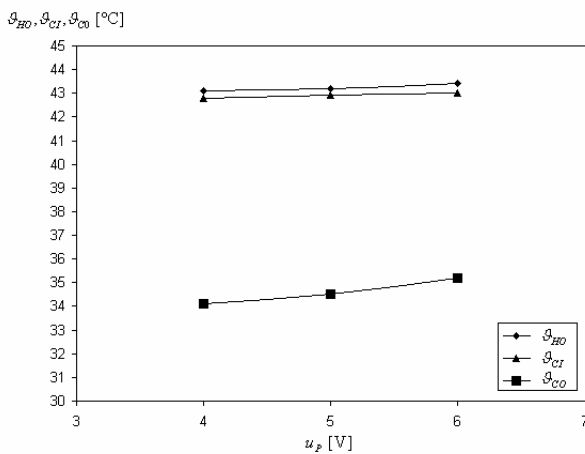


Fig.8 – Static characteristics  $\vartheta_{HO}(u_p)$ ,  $\vartheta_{CI}(u_p)$ ,  $\vartheta_{CO}(u_p)$ , for  $P = 300 \text{ W}$ ,  $u_c = 3 \text{ V}$ ,  $\vartheta_A = 24^\circ\text{C}$

Static characteristics  $\vartheta_{HO}(u_c)$ ,  $\vartheta_{CI}(u_c)$ ,  $\vartheta_{CO}(u_c)$  are in Fig. 9, for  $P = 300 \text{ W}$ ,  $u_p = 5 \text{ V}$ ,  $\vartheta_A = 24^\circ\text{C}$ , and relations  $\vartheta_{HO}(P)$ ,  $\vartheta_{CI}(P)$ ,  $\vartheta_{CO}(P)$  are depicted in Fig. 10, for  $u_p = 5 \text{ V}$ ,  $u_c = 3 \text{ V}$ ,  $\vartheta_A = 24^\circ\text{C}$ .

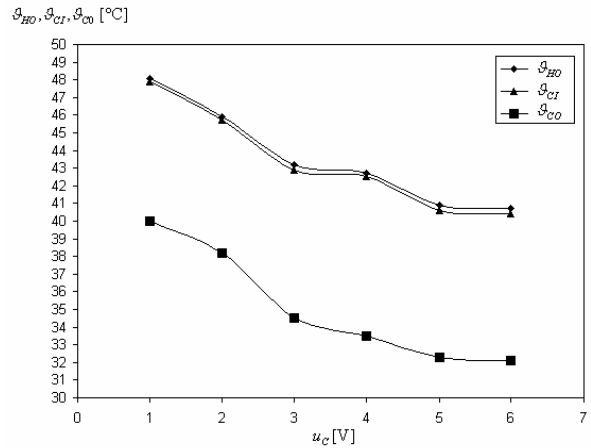


Fig.9 – Static characteristics  $\vartheta_{HO}(u_c)$ ,  $\vartheta_{CI}(u_c)$ ,  $\vartheta_{CO}(u_c)$ , for  $P = 300 \text{ W}$ ,  $u_p = 5 \text{ V}$ ,  $\vartheta_A = 24^\circ\text{C}$

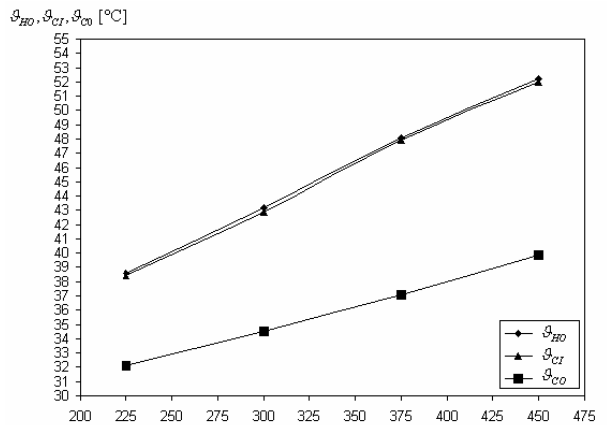


Fig.10 – Static characteristics  $\vartheta_{HO}(P)$ ,  $\vartheta_{CI}(P)$ ,  $\vartheta_{CO}(P)$ , for  $u_p = 5 \text{ V}$ ,  $u_c = 3 \text{ V}$ ,  $\vartheta_A = 24^\circ\text{C}$

The figures demonstrate the very good linearity of the model.

### 5.5 Delays estimation

Delays were estimated graphically from dynamic data (step responses) for appropriate system input changes; see Fig. 4 (B). The delay of the control action of the heat exchanger (cooler),  $\tau_{KC}$ , was obtained from the cooling curve (not displayed here). Results are dependent on the particular mass flow rate; as it can be seen from Table 7.

Table 7 - Measured delays as functions of  $u_p$

$u_p$ [V]	2	3	4	5	6
$\tau_H$ [s]	3	3	3	3	3
$\tau_{HC}$ [s]	125	125	120	110	105
$\tau_C$ [s]	24	23	22	21	20
$\tau_{KC}$ [s]	14	13	12	12	11
$\tau_{CH}$ [s]	10	10	9	9	8

Since the model does not reflect the influence of  $u_p$  upon the delays, arithmetical mean was taken in the final (i.e. for  $u_p = 4\text{ V}$ ). Delay in the heater,  $\tau_H$ , is short enough so that it can be omitted in the model, if one wants to.

$$\tau_H = 3\text{s}, \tau_{HC} = 110\text{s}, \tau_C = 22\text{s}, \tau_{KC} = 12\text{s}, \tau_{CH} = 9\text{s} \quad (18)$$

### 5.6 Masses estimation

Overall masses of water in the heater, the cooler and in the long pipeline were estimated graphically and numerically from dynamic characteristics, so that measured and calculated model give a good agreement. They influence mainly "slopes" of the steepest ascents in the particular step responses. For example,  $M_H$  influences the initial slope of the step response of  $P(t)$  to  $\vartheta_{HO}(t)$  mainly. An initial estimation had been made by graphical comparison of (model) simulated and measured responses

Final results obtained by the evaluation of the least mean squares criterion are the following

$$M_H = 0.08\text{ kg}, M_P = 0.22\text{ kg}, M_C = 0.27\text{ kg} \quad (19)$$

The final comparison of measured step responses and the calculated ones is depicted in Fig.11.

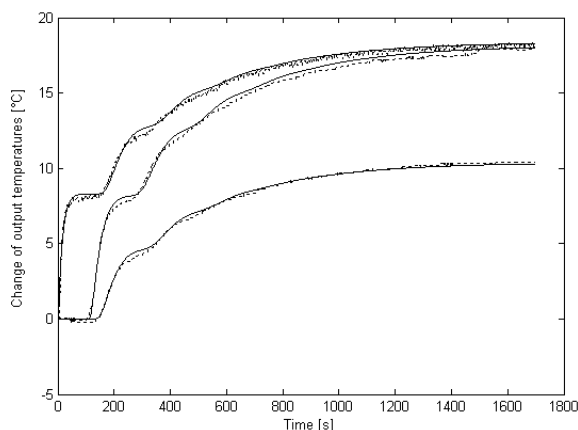


Fig.11 – Comparison of measured (dotted) and calculated (solid) step responses for the settings  $u_p = 5\text{ V}$ ,  $u_c = 3\text{ V}$ ,  $\Delta P = 300\text{ W}$ , on/off fan is on

## 6 Conclusions

The presented contribution studied a laboratory thermal heating model. The aim of the paper was to find a mathematical model of the appliance. In order to avoid needlessly complicated description, we utilized anisochronic modelling philosophy

comprising delays as an important factor in the plant dynamics; hence the model exhibits both the input-output and internal delays. Unknown parameters were further estimated experimentally and numerically in two steps: First, static characteristics gave rise to the static parameters such as heat transmitting coefficients, second, dynamic parameters such as delays or masses were estimated from step responses. The final graphical comparison of the step responses records a very good agreement of measured and calculated data.

The final results will be used for the verification of control algebraic algorithms developed by authors, in the future research.

## Acknowledgement

This work was supported by the grant of Ministry of Education, Sports and Youths of the Czech Republic, MSM 708 835 2102.

### References:

- [1] L. Hacia, K. Domke, Integral Modeling and Simulation in Some Thermal Problems, In: *Proceedings of the 5th IASME/WSEAS Int. Conference on Heat Transfer, Thermal Engineering and Environment*, Athens, Greece, August 25-27, 2007, pp. 42-47.
- [2] J. Krope, D. Dobersek and D. Goricaneč, Flow Pressure Analysis of Pipe Networks with Linear Theory Method, In: *Proceedings of the 2006 WSEAS/IASME International Conference on Fluid Mechanics*, Miami, Florida, USA, January 18-20, 2006.
- [3] L. Garbai, L. Barna, Modelling of non-steady-state conditions in a gas boiler heated room. In: *Proceedings of the 3<sup>rd</sup> IASME/WSEAS Int. Conf. on Heat Transfer, Thermal Engineering and Environment*, Corfu, Greece, August 20-22, 2006, pp. 6-11.
- [4] F. M. Koumboulis, N. D. Kouvakas and P. N. Paraskevopoulos, Analytic Modeling and Metaheuristic PID Control of a Neutral Time Delay Test Case Central Heating System, *WSEAS Trans. on Systems and Control*, Vol. 3, No. 11, 2008, pp. 967-981. ISSN: 1991-8763.
- [5] R. Bellman, K. L. Cooke, *Differential-difference equations*, Academic Press, New York, 1963.
- [6] P. Zítek, Anisochronic modelling and stability criterion of hereditary systems, *Problems of Control and Information Theory*, Vol. 15, No. 6, 1986, pp. 413-423.

- [7] P. Zítek, A. Víteček, *The design of control of subsystems with delays and nonlinearities* (in Czech). Prague, Czech Republic, ČVUT publishing, 1999.
- [8] W. Findeisen, J. Pulaczewski and A. Manitius, Multilevel optimization and dynamic coordination and dynamic coordination of mass flows in a beet sugar plant, *Automatica*, Vol. 6, 1970, pp. 581-589.
- [9] J. Morávka, K. Michálek, Anisochronous model of the metallurgical RH Process, Transactions of the VŠB – Technical University of Ostrava, Mechanical Series, Vol. 14, No. 2, 2008, pp. 91–96.
- [10] P. Dostálek, J. Dolinay and V. Vašek, Design and Implementation of Portable Data Acquisition Unit in Process Control and Supervision Applications, *WSEAS Trans. on Systems and Control*, Vol. 3, No. 9, 2008, pp. 779-788. ISSN: 1991-8763.
- [11] L. Pekař, R. Prokop, A simple stabilization and algebraic control design of unstable delayed systems using meromorphic functions, In: *Proceedings of the 26th IASTED International Conference MIC 2007*, Innsbruck, Austria, 2007, pp. 183-188. ISBN 978-0-88986-633-1.
- [12] L. Pekař, Parameterization-based control of anisochronic systems using RMS ring, *Transactions of the VŠB – Technical University of Ostrava, Mechanical Series*, Vol. 13, No. 2, 2007, pp. 93- 100. ISBN 978-80-248-1668-5.
- [13] J. Mareš, Simplified First Principle of Thermal Process, *XXXIIIrd Seminary ASR '2008*, VŠB-TUO, Ostrava, 2008, pp. 213–220.